Molecular Biology of the Cell
Vol. 12, 2567–2577, September 2001

Video Essay

ASH1 mRNA Localization in Three Acts[V]

Dale L. Beach* and Kerry Bloom

Department of Biology, University of North Carolina, Chapel Hill, North Carolina 27599-3280

Submitted February 27, 2001; Revised June 1, 2001; Accepted June 27, 2001
Monitoring Editor: Douglas Koshland

Novel green fluorescent protein (GFP) labeling techniques targeting specific mRNA transcripts reveal discrete phases of mRNA localization in yeast: packaging, transport, and docking. In budding yeast, *ASH1* mRNA is translocated via actin and myosin to the tip of growing cells. A GFP-decorated reporter transcript containing the *ASH1* 3′ untranslated region $gRNA_{ASH1}$ forms spots of fluorescence localized to a cortical domain at the bud tip, relocates to the mother-bud neck before cell separation, and finally migrates to the incipient bud site before the next budding cycle. The correct positioning of the mRNA requires at least six proteins: She1p-5p and Bud6p/Aip3p. $gRNA_{ASH1}$ localization in mutant strains identified three functional categories for the She proteins: mRNA particle formation (She2p and She4p), mRNA transport into the bud (She1p/Myo4p and She3p), and mRNA tethering at the bud tip (She5p/Bni1p and Bud6p/Aip3p). Because localization of the mRNA within the bud does not a priori restrict the translated protein, we examine the distribution of a mother-specific protein (Yta6p) translated from a mRNA directed into the bud. Yta6p remains associated with the mother cortex despite localization of the mRNA to the bud. This video essay traces the life history of a localized mRNA transcript, describes the roles of proteins required to polarize and anchor the mRNA, and demonstrates at least one instance where mRNA localization does not effect protein localization.

INTRODUCTION

Since the first description of asymmetrically distributed actin mRNA in ascidian embryos (Jeffrey *et al.*, 1983), localized transcripts have been identified in organisms from mice to men, frogs to flies, and most recently plants and fungus. The classic examples of localized messages primarily include embryonic polarity determinants: *oskar*, *bicoid*, *nanos*, and other mRNAs strategically positioned to define the primary axes of the *Drosophila* oocyte; Vg1 and other messages enriched in the vegetal hemisphere of the frog oocyte; and actin and myelin basic protein messages transported to specialized regions of highly polarized cells (St. Johnston, 1995). Most recently, *ASH1* mRNA localization to the bud tip in yeast (Long *et al.*, 1997; Takizawa *et al.*, 1997) and differential segregation of expansin mRNAs to apical and basipetal ends of xylem precursor cells (Im *et al.*, 2000) demonstrate that fungi and plants also asymmetrically distribute specific mRNA transcripts.

Live cell imaging of mRNA dynamics provides the opportunity to examine transport (path and rate) as well as anchorage (site and range) of mRNA in real time. Green fluorescent protein (GFP) labeling of nucleic acids is mediated through site-specific DNA or RNA binding proteins. The *Escherichia coli* transcriptional regulatory elements for the lactose operon (*lacI* and *lacO*) and the tetracycline operon (*tetR* and *tetO*) have been used as markers for chromosomal movements (Robinett *et al.*, 1996; Michaelis *et al.*, 1997). In parallel to DNA binding proteins, GFP fusions with site-specific RNA binding proteins are being used to visualize and track mRNA in living cells. Three investigators have independently constructed systems for the in vivo imaging of mRNA in live yeast cells. Two systems use the RNA binding coat protein (CP) of the bacteriophage MS2 (Bertrand *et al.*, 1998; Beach *et al.*, 1999) and a third uses the U1A splicing protein (Takizawa and Vale, 2000). Additionally, the MS2 coat protein-based system has been successfully applied to mammalian cells to image mRNA transport in living neurons (Rook *et al.*, 2000).

The localization of *ASH1* mRNA in budding yeast has provided an informative model system for mRNA transport and anchorage, combining live cell imaging, biochemistry, and genetics. Ash1p is a transcription factor that is segregated to the daughter cell nucleus providing an asymmetric cell fate determinant. The ability of haploid yeast cells to change mating types (**a** to α and/or α to **a**) is observed in mother cells; new daughter cells rarely switch mating type. Ash1p inhibits mating type switching in daughter cells by blocking HO endonuclease transcription (Bobola *et al.*, 1996; Maxon and Herskowitz, 2001; Sil and Herskowitz, 1996). Cleavage of the HO endonuclease site at the mating type locus initiates mating type switching. A separate activity of Ash1p is required for cells to enter unipolar (pseudohyphal) growth (Chandarlapaty and Errede, 1998). Ash1p asymme-

[V] Online version of this article contains video material for Figures 2–7. Online version available at www.molbiolcell.org.

*Corresponding author. E-mail address: dbeach@email.unc.edu.

Table 1. Yeast strains used in this work

Strain	Genotype	Reference
YEF473A	*MAT***a** *trp-Δ63, leu2Δ1, ura3-52, his3Δ200, lys2-8Δ1*	Bi *et al.* (1998)
JZY1345	*MATα trp1-Δ63, leu2Δ1, ura3-52, his3Δ200, lys2-8Δ1,* bud6Δ::TRP1	Amberg *et al.* (1997)
KBY1011	*MAT***a** *trp-Δ63, leu2Δ1, ura3-52, his3Δ200, lys2-8Δ1,* bni1Δ::LEU2	Beach *et al.* (1999)
KBY1012	*MATα, lys2, his3, ura3-52, leu2, myo4::ura3-52, ben*^{s}	Beach *et al.* (1999)
KBY1018	*MAT***a** *trp-Δ63, leu2Δ1, ura3-52, his3Δ200, lys2-8Δ1,* she2Δ::HPH	This study
KBY1019	*MAT***a** *trp-Δ63, leu2Δ1, ura3-52, his3Δ200, lys2-8Δ1,* she4Δ::HPH	This study
KBY1020	*MAT***a** *trp-Δ63, leu2Δ1, ura3-52, his3Δ200, lys2-8Δ1,* she4Δ::HIS3, she2Δ::HPH	This study
KBY1021	*MAT***a** *trpΔ63, leu2Δ1, ura3-52, his3Δ200, lys2-8Δ1,* she4Δ::HIS3	This study
KBY1027	*MAT***a** *trp-Δ63, leu2Δ1, ura3-52, his3Δ200, lys2-8Δ1,* yta6Δ::KAN	This study
KBY1046	*MAT***a** *trp-Δ63, leu2Δ1, ura3-52, his3Δ200, lys2-8Δ1,* bni1Δ::LEU2, bud6Δ::TRP1	This study

try requires a set of proteins originally identified as regulators of HO endonuclease expression (Bobola *et al.*, 1996; Jansen *et al.*, 1996; Sil and Herskowitz, 1996). *SHE1-SHE5* (for Swi5-dependent *HO* expression) regulates HO production, ultimately through the localization of the *ASH1* mRNA.

Daughter-specific inheritance of Ash1p is maintained by localizing the *ASH1* mRNA to the bud. Domains within the coding region and the 3′ untranslated region (UTR) of the *ASH1* mRNA encode signal sequences directing mRNA transport and anchorage within the bud (Chartrand *et al.*, 1999; Gonzalez *et al.*, 1999). Functional analyses of the *she* mutants have defined the steps in mRNA localization. In the absence of an individual She protein, the *ASH1* mRNA remains within the mother cell (*she1/myo4*), relocalizes to the neck (*she5/bni1*), or is distributed between the mother and the bud (*she2*, *she3*, *she4*).

Diffusion of proteins or mRNA from the bud into the mother may be inhibited at the neck via a barrier maintaining asymmetries between mother and bud. A genomic DNA array screen probing for additional transcripts associated with the She proteins (She1p/Myo4p, She2p, She3p) identified several genes, including *IST2* (Takizawa *et al.*, 2000). The *IST2* mRNA is localized in a *SHE1-5*-dependent manner, similar to the *ASH1* transcript, and Ist2p is predicted to be an integral membrane protein, restricted to the bud cortex by a septin-dependent barrier at the mother-bud neck (Takizawa *et al.*, 2000). The septin barrier restricts several proteins, including Spa2, Myo2p, Sec3p, and Sec5p to the bud and maintains actin patch asymmetry (Barral *et al.*, 2000). The presence of a septin-dependent barrier at the mother-bud neck delineates mother and bud cortical regions by maintaining the distribution of proteins between compartments. Potentially, such a barrier at the neck could inhibit the flow of both cortical and cytoplasmic factors, including proteins and mRNA.

The power of yeast genetics, combined with recent advances in multimode fluorescence microscopy, facilitates the dissection of the mRNA localization pathway. Once exported from the nucleus, *ASH1* mRNA transcripts coalesce into particles. Assembled particles are transported from the mother into the bud via actin cables, and once in the bud, the mRNA is constrained to the bud tip. We present a series of time-lapse sequences with this article to document aspects of mRNA dynamics in live cells.

MATERIALS AND METHODS

Growth Media and Yeast Strains

Wild-type cells were grown in YPD (2% glucose, 1% yeast extract, 2% peptone). Cells transformed with plasmids were grown on selective synthetic glucose based media (SD: 0.67% yeast nitrogen base, 2% glucose) lacking uracil, histidine, or both. To induce CP-GFP, CP/FG-GFP, GFP-Yta6, or GFP-Yta6-ASH1 production from pCP-GFP, pCP/FG-GFP, pGFP-YTA6, or pDB100, respectively, cells were switched to SD-MET for 1–2 h.

The strains used in these studies are listed in Table 1. Gene deletions were constructed by polymerase chain reaction (PCR) fragment-mediated transformation to replace the coding region of the target gene with a selectable marker as noted in Table 1 (Wach *et al.*, 1994). Deletions were verified by PCR with the use of primers flanking the coding region. Deletion and verification primer sequences are available upon request.

For live-cell imaging, cells were transferred onto growth chambers mounted on glass slides. Chambers were constructed as described in Shaw *et al.* (1997) with the use of SD-COMPLETE (synthetic dextrose media with a complete complement of nutritional supplements) or SD-MET (used to maintain induction from plasmids as listed above) supplemented with 0.25% gelatin (catalog no. G-2500; Sigma, St. Louis, MO). Mid-log phase cultures (OD_{660} = ~0.4–0.8) were concentrated ~20–50-fold before cells were added to the growth chamber. To arrest and maintain cells with large buds, cells were treated with 100 μM nocodazole to inhibit mitosis. Cells were arrested for 4 h before the induction of GFP-YTA6-ASH1. Because the *ASH1* mRNA localization is microtubule-independent, it is not affected by nocodazole treatments (Long *et al.*, 1997; Takizawa *et al.*, 1997).

To determine the frequency of green RNA (gRNA) spots within cell populations we observed cells of different genotypes (Table 2) coexpressing pIIIA/ASH1-UTR and pCP/FG-GFP. Cells grown to mid-log phase (OD_{660} = ~0.4–0.8) in SD-URA-HIS were washed in SD-MET, resuspended in 2 volumes of SD-MET, and incubated for 1 h at 30°C to induce production of the MS2-CP/FG-GFP fusion protein before observation. Cells were placed onto microscope slides pretreated with 0.1% poly-L-lysine to minimize movements during observations. The proportion of cells containing fluorescent spots within the population was determined by direct observation.

To determine whether the MS2 binding site (AAACATGAGGATTACCCATGT) is present within the *Saccharomyces cerevisiae* genome, the nucleotide sequence of the MS2 sites was submitted to a Blast search of the entire yeast chromosomal genome with the use of default settings (http://genome-www2.stanford.edu/cgi-bin/SGD/nph-blast2sgd). No hits were reported from a search completed January 25, 2001 (database posted September 13, 2000).

Plasmid Construction

The gRNA labeling system uses the plasmids pCP-GFP, containing a fusion between the MS2 coat protein and GFP, and a pIIIA/MS2-1-derived plasmid (SenGupta *et al.*, 1996) containing the *ASH1* 3′ UTR. $gRNA_{ASH1}$ imaging required plasmids pCP-GFP and pIIIA/ASH1-UTR (Beach *et al.*, 1999). $gRNA_{KAR9}$ imaging required pCP-GFP and pIIIA/K9UTR (Beach *et al.*, 1999). The plasmid pGFP-YTA6 is a generous gift of Don Katcoff (Bar Illam University, Ramat Gan, Israel), and includes an expression cassette for the green fluorescent protein fused to the amino terminus of the full-length *YTA6* coding region expressed from the *MET25* promoter.

The plasmid pCP/FG-GFP was constructed in a similar manner to pCP-GFP (Beach *et al.*, 1999). Briefly, the MS2 coat protein dlFG allele (Peabody and Ely, 1992) was amplified from pCT14-MS2-GFP (Bertrand *et al.*, 1998) via PCR and ligated into the *Bam*HI-*Xba*I sites of pUG23. The dlFG allele of the MS2 coat protein is deleted for the FG loop required for oligomerization of the protein and viral capsid formation (Peabody and Ely, 1992). Cells coexpressing CP-GFP and the MS2-ASH1 3′ UTR transcript were indistinguishable from cells coexpressing CP/FG-GFP and the MS2-ASH1 3′ UTR transcript (our unpublished results).

To construct pDB100, a PCR fragment containing the MS2 binding sites and E3 portion (Chartrand *et al.*, 1999) of the *ASH1* 3′ UTR from pIIIA/ASH1-UTR was generated. The fragment was cut with *Eco*RI at a site adjacent to the MS2 coat protein target sequence, which was filled in via Klenow polymerase to form a blunt end, and *Hin*dIII at a site incorporated into the downstream primer. The cut fragment was ligated into pGFP-YTA6 cut within the polylinker region downstream of the *YTA6* coding region at *Sma*I and *Hin*dIII sites to create the plasmid pDB100. pDB100 therefore contains an expression cassette for the GFP-YTA6-ASH1/E3 fusion construct regulated by the *MET25* promoter.

Microscopy and Image Processing

Microscopy and digital imaging, including optical sectioning, was performed as described in Shaw *et al.* (1997). Five optical sections, images taken at different focal planes ranging through the cell, were taken at 0.75-μm increments through the cell for a total of 3.0 μm/time point. The central optical section, including both a transmitted light and an epifluorescent (GFP) image was focused at the cell neck. Images were captured with the use of a Hamamatsu Orca II (model C4742-98) charge-coupled device camera mounted on a Nikon Eclipse E600FN with the use of 100× 1.4 NA Plan Apochromat objective with 1× magnification to the camera. The Metamorph software package (Universal Imaging, Downington, PA) for the Windows operating system was used for microscope automation, image acquisition, and image analysis. Images for publication were manipulated for scaling, size, resolution, and arrangement with Windows versions of Photoshop (Adobe Systems, Mountain View, CA) and Corel Draw (Corel, Ottawa, ON, Canada). Composite images of cells were generated with the use of the "3D Reconstruction" function of Metamorph set for a single plane construction with the use of the brightest elements from each image.

$gRNA_{ASH1}$ velocity measurements were obtained measuring the point-to-point movements of the $gRNA_{ASH1}$ spots. The distance of spot movements at 1-min intervals provided instantaneous velocities representing a minimal speed at each time point, and averaged over time. Only movements between sequential images were considered for velocity measurements. Because the spots frequently change direction between long time points, continuous velocities could not be measured.

RESULTS AND DISCUSSION

In Vivo mRNA Labeling

To construct an in vivo labeling system for mRNA, we used the site-specific RNA binding coat protein of the bacteriophage MS2. MS2 is a + strand RNA bacteriophage infecting F^+ *Escherichia coli* by binding the pili, rod-like extensions from the cell body. Late in the infection cycle, the coat protein binds MS2 genomic RNA preventing translation of the Replicase and coat protein genes, while allowing translation of the Lysis gene. These events precede complete encapsulation of the MS2 RNA genome by the coat protein, and lysis of the bacterial cell (Brock *et al.*, 1994). The MS2 binding site is a 23-bp sequence (5′-AAACAUGAGGAUUACCCAUGU-3′) that forms a stem loop structure bound by a homodimer of the coat protein (Peabody, 1990). Placement of the binding site adjacent to a start codon is sufficient to block translation initiation in both bacteria (Peabody, 1990) and budding yeast (Stripecke *et al.*, 1994) when bound by the coat protein. The MS2 coat protein binding site is absent from the *S. cerevisiae* genome (see MATERIALS AND METHODS), making integrated binding sites unique such that the MS2 coat protein recognizes only recombinant mRNA transcripts containing the MS2 coat protein binding site. The mRNA labeling system consists of two components (Figure 1): a recombinant RNA transcript, including "Your Favorite Gene" with two tandem MS2 binding sites, and a fusion protein combining the MS2 coat protein and the green fluorescent protein (Beach *et al.*, 1999).

The 3′ UTR of the *ASH1* mRNA encodes signal sequences sufficient for mRNA transport and anchorage within the bud. Unlike other localized mRNAs, the coding region of the *ASH1* message also includes targeting sequences capable of localizing the mRNA (Chartrand *et al.*, 1999; Gonzalez *et al.*, 1999). Our studies use a reporter construct, including two tandem repeats of the MS2 binding sites and the entire *ASH1* 3′ UTR (Beach *et al.*, 1999). Expression of the MS2-*ASH1* 3′ UTR fusion from a constitutively active promoter (RNA polymerase III-specific) allows the visualization of a localized reporter transcript throughout the cell cycle.

The MS2 coat protein fusion with GFP (CP-GFP) produces a fluorescent protein targeted to the recombinant transcript (Figure 1). Expression of CP-GFP alone results in a diffuse distribution of GFP fluorescence throughout the cytoplasm (Beach *et al.*, 1999). Attenuation of the CP-GFP fusion protein production via a regulated promoter (the *MET25* promoter) reduces background fluorescence within the cell. Coexpression of the MS2-*ASH1* 3′ UTR transcript with CP-GFP results in spots of GFP fluorescence localized to the bud tip (Figures 1 and 2). Termed gRNA, these $gRNA_{ASH1}$ spots localize as predicted from in situ labeling of *ASH1* mRNA in fixed cells (Long *et al.*, 1997; Takizawa *et al.*, 1997).

gRNA Localization in Wild-Type Cells

$gRNA_{ASH1}$ spots are clearly visible at the bud tip during bud growth (Figure 2, a and b), and $gRNA_{ASH1}$ spots are motile within a small domain at the bud tip in time-lapsed images of the cells (video sequence 1). Sequential images taken through the cell at 0.75-μm intervals indicate that the $gRNA_{ASH1}$ spots remain associated with the cell cortex and spots remain within ~0.3 μm of the bud tip. Spot movements within this region appear to be random because $gRNA_{ASH1}$ spots frequently move only short distances before changing direction, even when imaged at three frames per second (our unpublished results). The average movement rate of the spot at the bud tip is 0.3 μm/min (n = 10) (Beach *et al.*, 1999).

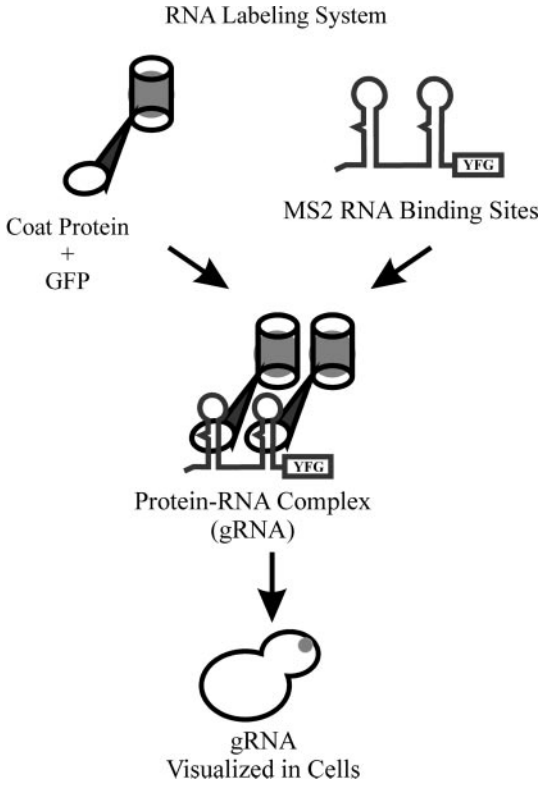

Figure 1. RNA labeling system. The RNA labeling system is comprised of two components: a site-specific RNA binding protein fused to GFP and an mRNA transcript containing the target sequence for the RNA binding protein. This system uses the MS2 coat protein and the associated RNA binding site. A mRNA transcript including "Your Favorite Gene" (YFG) and the MS2 coat protein binding site is fluorescently labeled when coexpressed with the MS2 coat protein fused to GFP. Localized transcripts can be visualized by standard fluorescence microscopy.

Late in the cell cycle, after cessation of bud growth and before cell separation, the $gRNA_{ASH1}$ relocalizes to the mother-bud neck. Migration of the $gRNA_{ASH1}$ toward the bud neck occurs 25 ± 5 min (n = 6) before cell separation (compare Figure 2, b and c; video sequence 1) and is more rapid than restricted movement at the bud tip, with velocities averaging ~1 μm/min (n = 4). $gRNA_{ASH1}$ at the neck remains motile, forming a single spot between the mother and bud domains. In a subset of cells, $gRNA_{ASH1}$ at the neck divides into independent spots in the mother and the bud (see video sequence 1). Spot separation precedes cell separation by ~10–15 min and correlates temporally with the completion of cytokinesis (Bi *et al.*, 1998). $gRNA_{ASH1}$ is then positioned at the incipient bud site for the ensuing cell cycle (Figure 2d; video sequence 1).

When presented with mating pheromones from cells of opposite mating type, yeast enter a period of highly polarized growth resulting in the formation of a mating projection or shmoo. Entry into the mating cycle and growth of the mating projection is another example of polarized growth in budding yeast. $gRNA_{ASH1}$ is localized at the tip of the mating projection before cell-cell contact, and remains at the isthmus between the cells after they fuse (Figure 3a, video

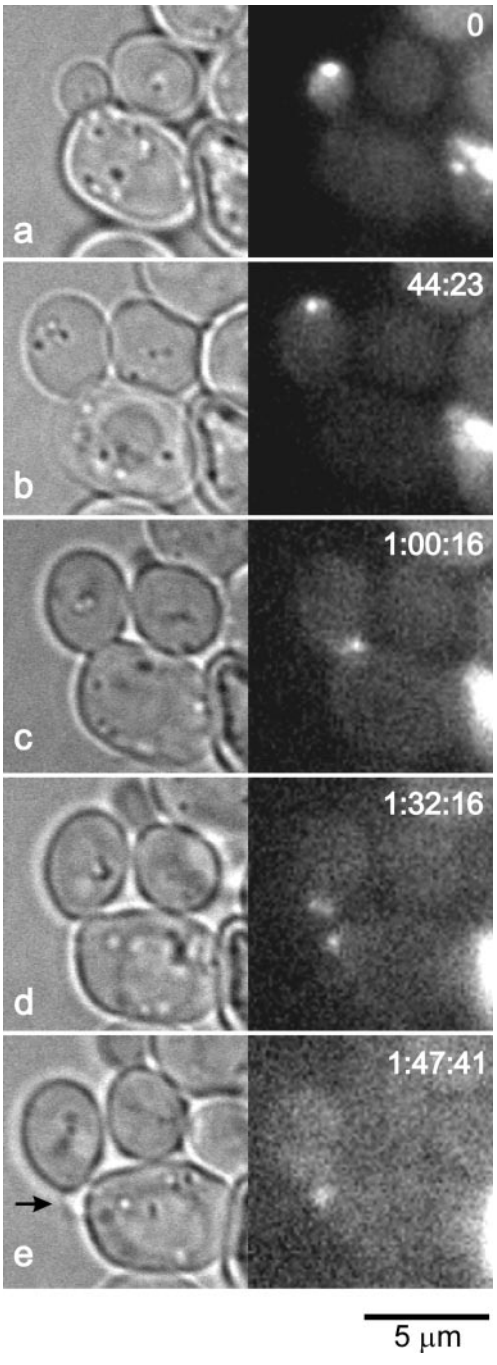

Figure 2. $gRNA_{ASH1}$ localization in vegetative, haploid cells. $gRNA_{ASH1}$ localization is dynamic, changing as the cell proceeds through the cell cycle. In small- (a) to large (b)-sized buds the $gRNA_{ASH1}$ is localized to the bud tip, moving on the cortex within a region at the bud tip termed the cortical bud cap. (c) $gRNA_{ASH1}$ migrates to the neck of large budded cells 25 min before cell separation. (d) After cell separation, the $gRNA_{ASH1}$ remains at the old bud site in both the mother and the bud. (e) Approximately 10 min before bud emergence (arrow) the $gRNA_{ASH1}$ moves to the incipient bud site then remains at the bud tip during early growth. Numbers in the upper right corner in each frame represent an elapsed time corresponding with video sequence 1. Bar, 5 μm.

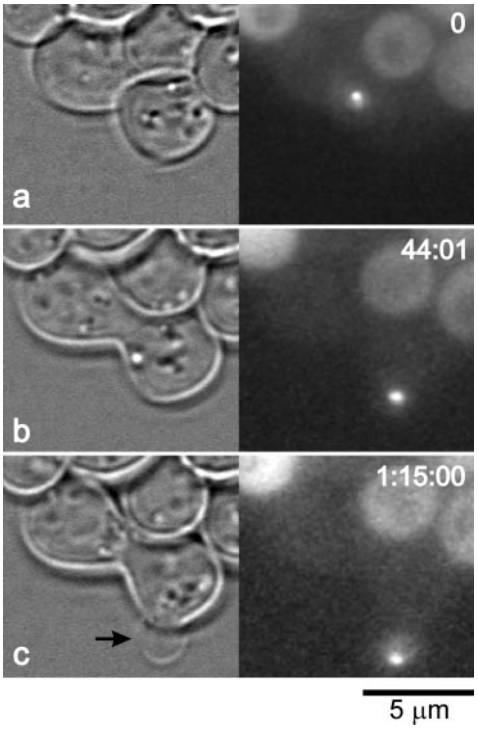

Figure 3. $gRNA_{ASH1}$ localization in mating cells. $gRNA_{ASH1}$ localizes to regions of polarized growth throughout the mating cycle. The two cells centered in the frame (*MATa* with $gRNA_{ASH1}$ is left, top and *MATα* is right, bottom) proceed through mating and generate a diploid bud. (a) Before cell fusion, the $gRNA_{ASH1}$ is at the mating projection tip nearest the cell of opposite mating type. The GFP signal in the left, top (*MATa*) cell is elevated compared with levels in the bottom, right cell (*MATα*). (b) After cell fusion and before bud emergence, the $gRNA_{ASH1}$ spot is localized at the incipient bud site (compare b and c). (c) $gRNA_{ASH1}$ is at the tip of the first diploid bud. Numbers in the upper right corner of each frame represent an elapsed time corresponding with video sequence 3. Bar, 5 μm.

sequence 2). One or more $gRNA_{ASH1}$ spots remain within proximity of the site of cell fusion, and retain motility, moving back and forth within the isthmus between the cells. $gRNA_{ASH1}$ localizes exclusively to the incipient bud site (compare Figure 3, a and b) ~20 min before emergence of the first diploid bud (Figure 3c).

The cell cycle-dependent localization of *ASH1* mRNA is similar to the transient localization of a number of polarity determinants (Pringle *et al.*, 1995), including Bni1p and Bud6p. Both proteins act to establish cell polarity through the actin cytoskeleton as well as to maintain *ASH1* mRNA localization (see below). Bni1p is localized to the site of cellular growth in the bud and returns to the neck before cell separation (Ozaki-Kuroda *et al.*, 2001). In contrast, Bud6p is distributed as punctate spots throughout the bud cortex, enriched at the bud tip and neck during cell growth, and forms two rings on mother and bud sides of the neck before cell division (Amberg *et al.*, 1997; Beach *et al.*, 1999; Segal *et al.*, 2000). Results from both vegetative and mating cells demonstrate that the *ASH1* mRNA is directed to sites of polarized growth.

Changes in the polarity of the actin cytoskeleton are mirrored in *ASH1* mRNA localization. Actin filaments reorient toward the neck concomitant with the completion of mitosis (Adams and Pringle, 1984), potentially in concert with the migration of Bni1p and Bud6p to the neck. Initially polarized toward the incipient bud site, the actin cytoskeleton remains polarized toward the bud tip through anaphase onset then reorients toward the neck before cytokinesis (Adams and Pringle, 1984), as observed for *ASH1* mRNA. The repositioning of anchored mRNA could be facilitated by transport along repolarized actin filaments, repositioned along with the cortical anchors She5p/Bni1p and Bud6p/Aip3p, or both.

she Mutants: Particle Formation

The initial step for mRNA localization is the packaging of transcripts into transport particles (Ainger *et al.*, 1993; Ferrandon *et al.*, 1994; Theurkauf and Hazelrigg, 1998; Wilhelm *et al.*, 2000). Although $gRNA_{ASH1}$ forms particles in wild-type strains, we observed a decrease in the number of cells containing $gRNA_{ASH1}$ spots in a *she2* mutant strain (Table 2; Bertrand *et al.*, 1998) and incomplete particle aggregation in both *she2* and *she4* cells (Figure 4). To be certain that spots observed in these strains were due to *ASH1* mRNA aggregation and not MS2 coat protein multimers, we detected the reporter transcript with the use of a modified coat protein (pCP/FG-GFP; see MATERIALS AND METHODS). A deletion of the FG loop in the dlFG allele of the MS2 coat protein inhibits protein-protein interactions required for oligomerization of the coat protein and viral capsid formation (Peabody and Ely, 1992). Expression of CP/FG-GFP in the absence of the reporter transcript produced fluorescent spots in <1% of the cells (Table 2, YEF473 pCP/FG-GFP). $gRNA_{ASH1}$ spots are observed in ~3.5% of *she2* cells, one-third fewer than an isogenic wild-type strain (Table 2). In a *she4* strain, cells containing $gRNA_{ASH1}$ spots are observed at frequencies similar to wild type (Table 2), whereas the frequency of cells containing fluorescent spots in the double mutant *she2 she4* are reduced to the value of the *she2* single mutant (Table 2).

In *she2* and *she4* mutant cells containing $gRNA_{ASH1}$ spots, multiple spots are observed, whereas wild-type cells maintain only one to two localized spots. Of time-lapsed cells, 67% of *she2* (n = 10) and 72% of *she4* (n = 18) cells contained three or more spots distributed between mother and bud (Figure 4, b and e; video sequences 3 and 4). The number of

Table 2. Spot formation frequencies
The proportion of cells containing one or more gRNA spots is shown for different strains defective in spot aggregation.

Strain	Spot Frequency (%)	n
YEF473A gRNA-FG (WT)	9.7 ± 2.1	995
KBY1018 gRNA-FG (*she2*)	3.5 ± 0.7	962
KBY1019 gRNA-FG (*she4*)	10.7 ± 3.2	1010
KBY1020 gRNA-FG (*she2*, *she4*)	3.7 ± 0.6	533
YEF473A pCP/FG-GFP	0.4 ± 0.2	917

WT, wild type.

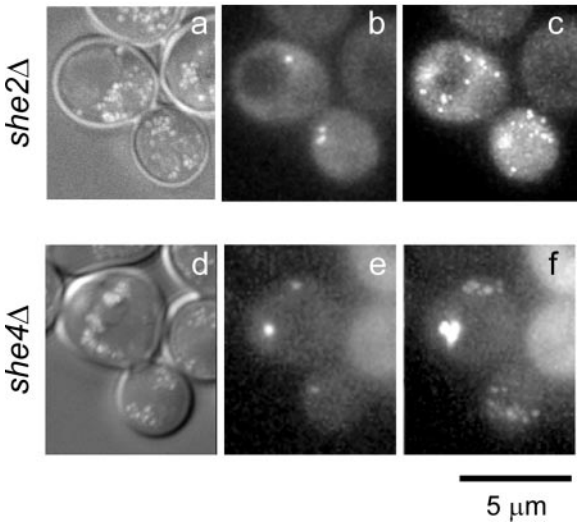

Figure 4. She2p and She4p are required for $gRNA_{ASH1}$ spot assembly. $gRNA_{ASH1}$ localization in *she2*Δ (a–c, g, and h), and *she4*Δ (d-f, i, and j) cells. (a–c) $gRNA_{ASH1}$ aggregates into spots in both the mother and the bud in *she2*Δ cells. A single *she2*Δ cell is shown imaged via DIC (a) and GFP fluorescence (b). The composite image (c) represents 20 consecutive time points at a 1-min interval to illustrate dynamic spot movements not apparent within single images (video sequence 3). (d–f) Several spots distributed between mother and but were also observed in *she4*Δ cells. A single *she4*Δ cell is shown imaged via Nomarski (a) and GFP fluorescence (b). The composite image (c) represents 20 consecutive time points at a 1-min interval to illustrate dynamic spot movements not apparent within single images (video sequence 4). Bar, 5 μm.

spots varied between cells, and a maximum of six independent, motile spots was observed in a single *she4* cell. Inspection of individual optical sections (see MATERIALS AND METHODS) reveals that the $gRNA_{ASH1}$ spots in either strain are not associated with the cell cortex. Spots observed in *she2*Δ and *she4*Δ cells were motile with average velocities of 0.93 ± 0.56 μm/min (n = 3) and 0.61 +/- 0.19 μm/min (n = 4), respectively. These rates are similar to *ASH1* mRNA in other *she* mutants (see below) and two- to threefold faster than spots at the bud tip in wild-type cells. To illustrate the distribution and movements of $gRNA_{ASH1}$ spots in *she2* and *she4* cells, multiple frames from each time lapse are combined to form the composite images shown in Figure 4, c and f. These images represent 15 consecutive images captured at 1-min intervals to demonstrate spot dynamics in a single image. The formation of multiple spots illustrates a loss of efficient *ASH1* mRNA packaging in the absence of She2p or She4p.

Binding of the *ASH1* mRNA by She2p likely initiates particle formation, yet a functional transport particle requires additional nuclear and cytoplasmic proteins. Whether She2p binds the mRNA within the nucleus or the cytoplasm remains unknown. The nuclear protein, Loc1p is a novel protein affecting *ASH1* mRNA localization (Long *et al.*, 2001). Although the *ASH1* mRNA is exported from the nucleus in *loc1* cells, the transcript is distributed throughout the cell, resulting in a *she* phenotype (Ash1p in mother and daughter nuclei). The diffuse appearance of the mRNA in *loc1* cells indicates an inability to form particles. Thus, Loc1p may facilitate mRNA folding or otherwise assist in loading She2p onto the *ASH1* transcript to initiate particle aggregation. She2p interactions with the nuclear importin Srp1p (Uetz *et al.*, 2000) implicates She2p binding of the *ASH1* mRNA within the nucleus before export or in conjunction with nuclear export of the transcript. The CP-GFP fusion used in these studies is capable of distinguishing between nuclear and cytoplasmic transcripts (Beach *et al.*, 1999). Because we did not detect a nuclear GFP signal in *she2* cells (Figure 4), She2p is apparently not required for nuclear export of the mRNA. Finally, She2p bound to the *ASH1* transcript is required for the recruitment of She3p and subsequently She1p/Myo4p to form a mature transport particle (Munchow *et al.*, 1999; Bohl *et al.*, 2000; Long *et al.*, 2000; Takizawa and Vale, 2000).

she4 mutants display defects in actin filament polarity, bud site selection, and endocytosis (Wendland *et al.*, 1996). She4p is distributed throughout the cytoplasm and does not colocalize with the *ASH1* mRNA, indicating that She4p does not specifically bind the *ASH1* mRNA (Bertrand *et al.*, 1998; Takizawa and Vale, 2000). Because perturbations of the actin cytoskeleton affect *ASH1* mRNA localization without disrupting $gRNA_{ASH1}$ particle formation (Long *et al.*, 1997; Takizawa *et al.*, 1997; Beach *et al.*, 1999; see below), the incomplete particle aggregation in *she4* mutants reflects additional complexities in efficient particle formation.

she Mutants: Motors and Motor Attachment

In the absence of She1p/Myo4p, a type V myosin, the $gRNA_{ASH1}$ is no longer transported into the bud, although transcripts assemble into a discrete spot and remain motile (Figure 5, a–c; video sequence 5). The single spot (Figure 5b) moves throughout the mother cell at an average velocity of ~0.6 μm/min (Beach *et al.*, 1999). The composite image (Figure 5c) illustrates the movement of the spot over a period of 20 min taken from 20 sequential frames (video sequence 5). Observation of individual optical sections taken at increments of 0.75 μm indicates that the gRNA is cytoplasmic, contrasting with the cortical localization of the gRNA spots in wild-type cells. Although $gRNA_{ASH1}$ mRNA particles were never observed to cross the mother bud neck, spots accumulate in the daughter cell late in the cell cycle (video sequence 5). The accumulation of $gRNA_{ASH1}$ in the bud presumably results from transcription within the daughter nucleus after anaphase.

Myo4p represents one of two class V myosins identified in budding yeast. Myo4p is suspected to have arisen from a gene duplication event of a second, class V myosin in yeast, *MYO2*, diverging in the globular tail domain (Haarer *et al.*, 1994). In contrast to the dedicated role of Myo4p in RNA transport, Myo2p is a multifunctional motor protein responsible for vesicular and vacuolar traffic (Pruyne and Bretscher, 2000) as well as the transport of Kar9p into the bud (Beach *et al.*, 2000; Yin *et al.*, 2000). Myo2p-dependent transport of Kar9-GFP follows actin cables from the mother to the bud at an average velocity of ~90 μm/min (Beach *et al.*, 2000). In contrast, the Myo4p-dependent transport of *ASH1* mRNA follows a nonlinear path at rates of 30 μm/min (Bertrand *et al.*, 1998). Transport via both motors requires actin filaments. Depolymerization of actin filaments in tropomyosin mutant cells inhibits Myo2p- and Myo4p-depen-

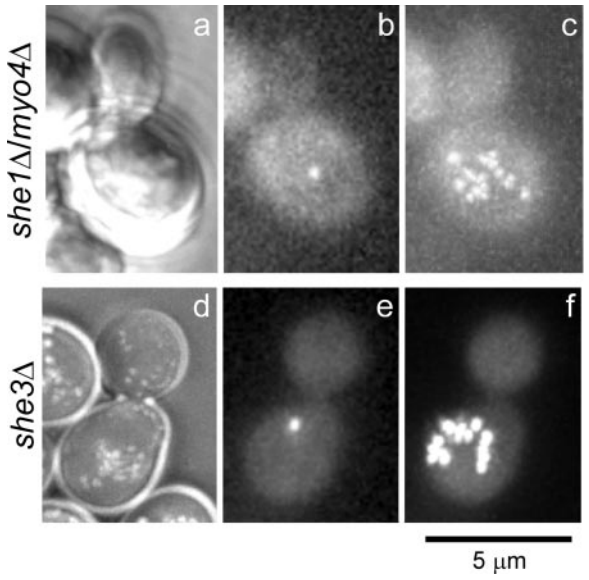

Figure 5. She1p/Myo4p and She3p facilitate $gRNA_{ASH1}$ transport. In the absence of either She1p/Myo4p or She3p, $gRNA_{ASH1}$ remains in the mother cell. (a–c) Nomarski (a), single time point (b), and composite image (c) of a *she1*Δ/*myo4*Δ cell are shown (video sequence 5). The single $gRNA_{ASH1}$ spot is centrally located within the mother. The composite image (c) demonstrates the spot motility in the absence of the myosin motor. Twenty sequential images >20 min are presented in the single composite image (see text). (d–f) Nomarski (d), single time point (e), and composite image (f) of a *she3*Δ cell are shown (video sequence 6). As seen for *she1* cells, the single $gRNA_{ASH1}$ spot is localized in the mother domain (below the bud). The composite image (f) represents 20 sequential images and the movement of a single spot >20 min. Bar, 5 μm.

dent transport (Long *et al.*, 1997; Pruyne *et al.*, 1998; Beach *et al.*, 2000).

Attachment of the $gRNA_{ASH1}$ to the myosin motor protein is mediated by She3p. Time-lapse images of $gRNA_{ASH1}$ spots in *she3* cells are similar to the *she1/myo4* strain (Figure 5, d–f; video sequence 6). $gRNA_{ASH1}$ spots are confined to the mother in *she3* cells and move at a velocity of 0.8 ± 0.2 μm/min, similar to $gRNA_{ASH1}$ in *she1/myo4* cells. A composite image (Figure 5f) illustrates the motility and range of the $gRNA_{ASH1}$ in the *she3* cells. Spots are cytoplasmic, as determined by observation of the optical sections, and new spots appear within the bud late in the cell cycle (video sequence 6) as seen in *she1/myo4* cells. Biochemical evidence supports a role for RNA loading onto She1p/Myo4p via She3p in association with She2p, and She1p/Myo4p and She3p form a complex in the absence of She2p or *ASH1* mRNA (Munchow *et al.*, 1999; Bohl *et al.*, 2000; Long *et al.*, 2000; Takizawa *et al.*, 2000). Because an RNA particle forms in the absence of She3p, inclusion of a She3p-She1p complex is not required for particle formation. Thus, She3p acts as an adapter between She1p/Myo4p with the *ASH1* transcript.

The myosin motor She1p/Myo4p tethers the *ASH1* mRNA particle to actin. Cortical association of the mRNA is lost when Myo4p is unable to bind the mRNA in *she1/myo4*, *she3*, and *she2* deletions. Thus, Myo4p, and the intervening proteins She2p and She3p serve as links connecting filamentous actin and the mRNA. Because particles formed in *she4* cells are cytoplasmic, She4p may contribute to the cortical association of the mRNA as well, potentially facilitating the cross talk between actin polarity and mRNA particle formation.

she Mutants: Polarity Markers and Cortical Anchorage

Anchorage of the $gRNA_{ASH1}$ at the bud tip requires both She5p/Bni1p and Bud6p. Previous reports indicated that the *ASH1* mRNA relocalized to the bud neck in fixed populations of *she5/bni1* cells (Long *et al.*, 1997; Takizawa *et al.*, 1997; Bertrand *et al.*, 1998). Subsequent live cell analysis revealed that the *ASH1* mRNA is localized to the bud in a *she5/bni1* strain but is not restricted to the bud tip as observed in wild-type cells (Beach *et al.*, 1999). The $gRNA_{ASH1}$ spot returns to the neck before cell separation, which may establish a stable position for the mRNA as observed in fixed cell analyses. A single time point from the time-lapse series shows that the $gRNA_{ASH1}$ can be positioned adjacent to the neck (Figure 6b). Figure 6c represents 20 sequential images over a period of 20 min and demonstrates the dynamic distribution of the RNA throughout the bud over time (video sequence 7). $gRNA_{ASH1}$ spots move throughout the bud in the absence of She5p/Bni1p and are not observed in the mother cell (Figure 6, b and c; video sequence 7). The $gRNA_{ASH1}$ spots remain associated with the cortex, as determined from individual optical sections taken at 0.75-μm intervals through the cell. The fluorescent spot moves on the bud cortex at ~0.5 μm/min (n = 4) (Beach *et al.*, 1999).

Live cell analysis of $gRNA_{ASH1}$ dynamics unveiled a sixth protein, Bud6p/Aip3p, required for proper *ASH1* mRNA localization (Beach *et al.*, 1999). Because both She5p/Bni1p and Bud6p/Aip3p are required to preserve cortical association of the microtubule anchor protein, Kar9p (Miller *et al.*, 1999; Beach *et al.*, 2000), we examined the role of Bud6p in the localization of *ASH1* mRNA. In the absence of Bud6p, $gRNA_{ASH1}$ spots move throughout the bud, remaining associated with the cortex as seen for *she5/bni1* cells (Figure 6, d–f; video sequence 8). A similar result is observed in *bni1 bud6* double mutants such that the $gRNA_{ASH1}$ spot remains associated with the cortex yet not restricted to the bud tip (our unpublished results). The motile spots have an average velocity of ~0.5 μm/min (Beach *et al.*, 1999). Figure 6e contains a single time point, where the $gRNA_{ASH1}$ spot is mislocalized to the neck, whereas Figure 6f is a composite image consisting of 20 consecutive frames representing 20 min. The composite images of *she5/bni1* and *bud6/aip3* cells demonstrate the continued motility of the $gRNA_{ASH1}$ and dynamic distribution in these cells that is not seen in wild type (compare Figure 6,c, f, and i).

Bni1p/She5 and Bud6p/Aip3p are bud-specific proteins that appear to act as cell polarity cues within the bud. Both proteins participate in diploid bud site establishment, actin polarity, and alignment of the mitotic spindle (Amberg *et al.*, 1997; Evangelista *et al.*, 1997; Lee *et al.*, 1999; Yeh *et al.*, 2000). In the absence of either Bni1p or Bud6p, the *ASH1* mRNA is released from a tight association at the bud tip. Although the actin cytoskeleton is disrupted in the *bni1* and *bud6* cells, the effect is not sufficient to inhibit directional transport of the message between the mother and bud. An intact linkage to the cortex, presumably through She3p and She4p (myosin V), indicates that Bni1p/She5p and Bud6p/Aip3p are not

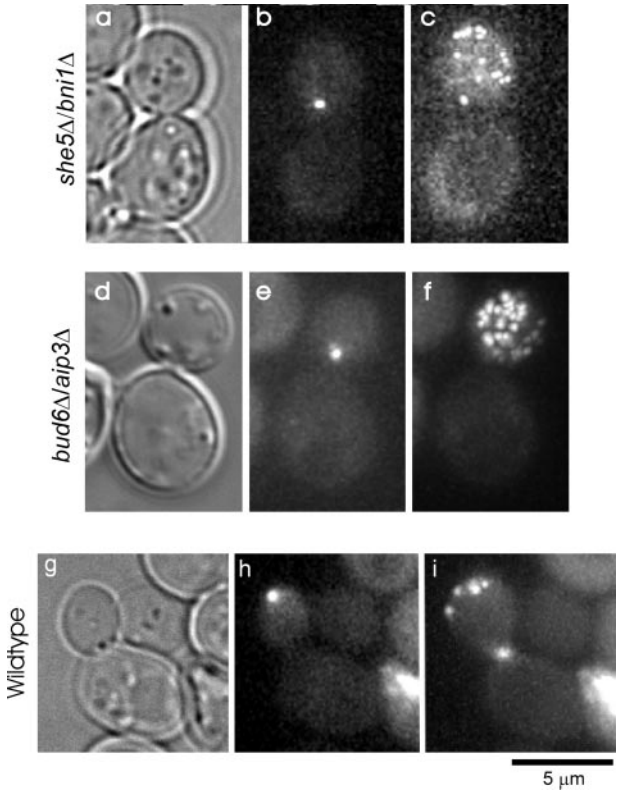

Figure 6. She5p/Bni1p and Bud6p/Aip3p anchor the $gRNA_{ASH1}$ at the bud tip. The retention of the $gRNA_{ASH1}$ at the bud tip is lost in *she5*Δ/*bni1*Δ and *bud6*Δ/*aip3*Δ cells. (a–c) In *she5*Δ/*bni1*Δ cells, the $gRNA_{ASH1}$ is transported into the bud and moves freely throughout the bud. (a) Brightfield image of the cell shown in b and c. (b) A single frame from the time lapse (video sequence 7) is shown, demonstrating a position of the $gRNA_{ASH1}$ proximal to the neck. (c) Composite time-lapse image is shown representing 20 sequential images, showing the distribution of the $gRNA_{ASH1}$ spot >20 min. (d–f) As observed for *she5*Δ/*bni1*Δ cells, $gRNA_{ASH1}$ is transported into the bud in *bud6*Δ/*aip3*Δ cells, and moves freely throughout the bud. (d) Brightfield image of the cell shown in e and f. (e) Single frame from the time lapse (video sequence 8) demonstrating a position of the $gRNA_{ASH1}$ proximal to the neck. (f) Composite time-lapse image is shown representing 20 sequential images showing the distribution of the $gRNA_{ASH1}$ spot >20 min. (g–i) Wild-type (YEF473a) cells are shown to compare $gRNA_{ASH1}$ localization distal from the neck (h) and as a composite image (i) representing 20 sequential images >20 min. (g) Brightfield image of the wild-type cell shown in h and i. Bar, 5 μm.

required for cortical interactions. Because both proteins populate the cortex at the bud tip (see above), mislocalization of the *ASH1* mRNA in *she5/bni1* or *bud6/aips* cells probably results from a loss of specific mRNA anchorage at the bud tip.

Bni1p/She5 and Bud6p/Aip3p also are required for localization of Kar9p to the bud cortex. Kar9p establishes microtubule and nuclear orientation early in the cell cycle by providing a polarized anchorage site for microtubules (Miller and Rose, 1998; Miller *et al.*, 1999; Beach *et al.*, 2000). In the absence of Kar9p, Bni1p, or Bud6p, the orientation and dynamics of the mitotic spindle are disrupted (Lee *et al.*, 1999; Yeh *et al.*, 2000). Although Kar9p is lost from the cortex in *bni1* and *bud6* cells, the *ASH1* mRNA remains cortical and maintains particle integrity (see above). In addition to Bni1p and Bud6p, Spa2p localizes to the bud tip and is required with Bud6p for Bni1p localization (Ozaki-Kuroda *et al.*, 2001). Taken together, these three proteins provide a nexus at the bud tip linking positional cues and asymmetric anchors.

mRNA Asymmetry Does Not Define Protein Localization

In addition to bud-specific proteins (i.e., Bni1p, Bud6p, Cdc42p, Sec3p, etc.), mother-specific proteins such as Yta6p have been identified. A screen for yeast orthologs of human proteosome constituents identified, among other genes, *YTA6* (Schnall *et al.*, 1994), a member of the AAA ATPase family (Vale, 2000). A GFP-Yta6 fusion protein forms punctate spots of fluorescence specifically on the mother cortex that are absent from the bud cortex of small and medium budded cells (Figure 7, a–e; video sequence 9). In cells with large buds, GFP-Yta6 begins to accumulate within the bud near the time of anaphase onset (Figure 7, a′–e′; video sequence 9). GFP-Yta6 first appears in the bud as small, dim spots, which increase in number and brightness with time. Spots remain relatively stationary in either mother or bud, appearing to move within small domains (video sequence 9). The localization of GFP-Yta6 was unchanged in cells deleted for the chromosomal *YTA6* locus (our unpublished results).

To determine the contribution of mRNA targeting versus peptide sequences for protein localization, we fused the *ASH1* 3′ UTR downstream of the *YTA6* coding region to direct mRNA into the bud. The fusion places the E3 domain of the *ASH1* 3′ UTR downstream of the GFP-Yta6, and includes MS2 sites to visualize the transcript. Expression of the GFP-YTA6-MS2-ASH1/E3 (referred to as GFP-Yta6-ASH1) fusion protein in unsynchronized, haploid cells resulted in a distribution of fluorescent spots similar to those seen for GFP-Yta6. The GFP-Yta6-ASH1 protein formed nonmotile, punctate spots of fluorescent throughout the mother cortex of unbudded, small, and medium budded cells, and accumulated in large budded cells (see Figure 7, g and h, for representative images).

To determine the localization of the GFP-Yta6-ASH1 fusion mRNA, we coexpressed the fusion protein with CP-GFP. Coexpression of both GFP fusion proteins in unsynchronized, haploid *yta6*Δ cells produced the wild-type distribution of GFP-Yta6 spots within the mother, and a single, bright spot at the bud tip (Figure 7f; video sequence 10). The fluorescent spot at the bud tip is exclusive within the bud and localized tightly to the bud tip. The fluorescent spot at the bud tip appears brighter than GFP-Yta6 on the mother cortex and was not observed in cells lacking CP-GFP. Late in the cell cycle, GFP-Yta6-ASH1 spots accumulate in the bud as observed for wild-type cells (Figure 7g; video sequence 10). Thus, directing the *YTA6* mRNA into the bud did not alter the mother specific localization of the protein.

The maternal localization of the GFP-Yta6-ASH1 fusion protein could result from protein expressed in the previous cell cycle. To evaluate the distribution a protein transcribed from a mRNA localized within the bud, we restricted ex-

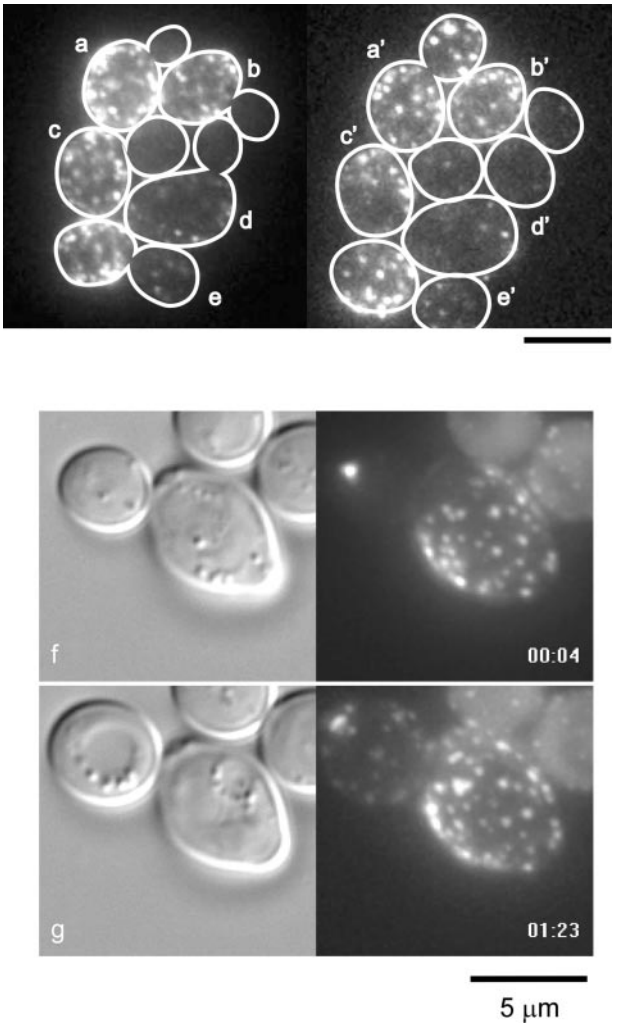

Figure 7. GFP-Yta6 localizes to the maternal cortex. (a–e) Several cells are shown with GFP-Yta6 spots on the mother cell cortex. Medium budded cells (a–d) contain GFP-Yta6 only in the mother cell, while the large budded cell (e) contains GFP-Yta6 in both mother and bud domains. (a′–e′) The same cells 150 min later. Cells b–e have completed cell separation with Yta6p present in the daughter cells. Cell a′ has not completed cell separation, yet Yta6p is localized in the bud. White lines denote the cell outline as determined from the brightfield image. Video sequence 9 demonstrates the accumulation of YTA6p in the bud late in the cell cycle and includes panels showing the nuclear cycle (Histone H4-CFP). (f and g) The localization of Yta6-ASH1 fusion protein and mRNA is shown in a cell expressing GFP-Yta6-*ASH1* 3′ UTR fusion and CP-GFP (video sequence 10). The mRNA is localized to the bud tip throughout the time lapse (f and g), whereas the Yta6-Ash1 fusion protein is only in the mother in small budded cells (f) and in both mother and bud in large budded cells (g). Numbers in the lower right corner (f and g) represent an elapsed time (hh:mm) corresponding with video sequence 10. Bars (top and bottom), 5 μm.

pression of the fusion protein to large budded cells. Cells were arrested at mitosis with large buds before GFP-Yta6-ASH1 induction (see MATERIALS AND METHODS). All of the cells observed contained GFP-Yta6-ASH1 fluorescent spots within the mother ($n > 500$), similar to wild-type GFP-Yta6. We conclude that the localization of the GFP-YTA6-ASH1 fusion protein is not altered by directing the mRNA to the bud tip.

The resulting position for Ash1p, GFP-YTA6, or GFP-YTA6-ASH1 is indicative of a hierarchy of peptide signals over RNA localization signal sequences. Transcription of *ASH1* late in the cell cycle and restricted translation of the protein to the bud results in the preferential accumulation of Ash1p in the daughter nucleus. However, Ash1p is equally competent to enter either nucleus, as evident upon overexpression of *ASH1.* Thus, in the absence of stringent regulation of mRNA localization and protein levels the protein accumulates in both nuclei. In contrast, the mother-specific localization of Yta6p is not affected by transcript localization. Localized mRNA translation therefore does not override the protein localization machinery.

Extensions of Live Cell Imaging

The extension of live cell imaging to the "RNA world" enables cell biologists to follow the path of mRNA transcripts in live cells. Whole genome screening and empirical observation have identified additional asymmetrically distributed transcripts, including a second bud-specific mRNA, *IST2* (Takizawa *et al.*, 2000), as well as nuclear messages targeted to the mitochondria (Corral-Debrinski *et al.*, 2000). Such facilitated placement of messages within the already compact yeast cell illustrates the biological importance of site-specific translation. Cross talk between cell polarity determinants and the mRNA localization pathway indicate synergy between mechanisms establishing cell polarity and mRNA localization. The coupling of these inherently asymmetric processes is likely to represent conserved features responsible for establishing asymmetries in development.

ACKNOWLEDGMENTS

We thank Elaine Yeh for critical reading of the manuscript, Ted Salmon (University of North Carolina, Chapel Hill, NC) for inspired guidance, David Peabody (University of New Mexico School of Medicine, Albuquerque, NM) and Roy Long (Medical College of Wisconsin, Milwaukee, WI) for providing plasmids carrying the MS2 CPdlFG allele, Don Katcoff (Bar Ilan University, Ramat Gan, Israel) and John Pringle (University of North Carolina, Chapel Hill, NC) for yeast strains, and Jennifer Stemple and Jennifer Mott for technical assistance. This work is supported by a National Institutes of Health Grant GM-32238 issued to K.B.

REFERENCES

Adams, A.E.M., and Pringle, J.R. (1984). Relationship of actin and tubulin distribution to bud growth in wild-type and morphogenetic-mutant *Saccharomyces cerevisiae*. J. Cell Biol. *98*, 934–945.

Ainger, K., Avossa, D., Morgan, F., Hill, S.J., Barry, C., Barbarese, E., and Carson, J.H. (1993). Transport and localization of exogenous myelin basic protein mRNA microinjected into oligodendrocytes. J. Cell Biol. *123*, 431–441.

Amberg, D.C., Zahner, J.E., Mulholland, J.W., Pringle, J.R., and Botstein, D. (1997). Aip3p/Bud6p, a yeast actin-interacting protein that is involved in morphogenesis and the selection of bipolar budding sites. Mol. Biol. Cell *8*, 729–753.

Barral, Y., Mermall, V., Mooseker, M., and Snyder, M. (2000). Compartmentalization of the cell cortex by septins is required for maintenance of cell polarity in yeast. Mol. Cell *5*, 841–851.

Beach, D.L., Salmon, E.D., and Bloom, K. (1999). Localization and anchoring of mRNA in budding yeast. Curr. Biol. *9*, 569–578.

Beach, D.L., Thibodeaux, J., Maddox, P., Yeh, E., and Bloom, K. (2000). The role of the proteins Kar9 and Myo2 in orienting the mitotic spindle of budding yeast. Curr. Biol. *10*, 1497–506.

Bertrand, E., Chartrand, P., Schaefer, M., Shenoy, S.M., Singer, R.H., and Long, R.M. (1998). Localization of *ASH1* mRNA particles in living yeast. Mol. Cell *2*, 437–445.

Bi, E., Maddox, P., Lew, D.J., Salmon, E.D., McMillan, J.H., Yeh, E., and Pringle, J.R. (1998). Roles of a nonessential actomyosin contractile ring and of the septins in *Saccharomyces cerevisiae* cytokinesis. J. Cell Biol. *142*, 1301–1312.

Bobola, N., Jansen, R.-P., Shin, T.H., and Nasmyth, K. (1996). Asymmetric accumulation of Ash1p in postanaphase nuclei depends on a myosin and restricts yeast mating-type switching to mother cells. Cell *84*, 699–709.

Bohl, F., Kruse, C., Frank, A., Ferring, D., and Jansen, R.P. (2000). She2p, a novel RNA-binding protein tethers ASH1 mRNA to the Myo4p myosin motor via She3p. EMBO J. *19*, 5514–5524.

Brock, T.D., Madigan, M.T., Martinko, J.M., and Parker, J. (1994). Biology of Microorganisms, 7th ed., Englewood Cliffs, NJ: Prentice Hall.

Chandarlapaty, S., and Errede, B. (1998). Ash1, a daughter cell-specific protein, is required for pseudohyphal growth of *Saccharomyces cerevisiae*. Mol. Cell Biol. *18*, 2884–2891.

Chartrand, P., Meng, X.-H., Singer, R.H., and Long, R.M. (1999). Structural elements required for the localization of *ASH1* mRNA and of a green fluorescent protein reporter particle *in vivo*. Curr. Biol. *9*, 333–336.

Corral-Debrinski, M., Blugeon, C., and Jacq, C. (2000). In yeast, the 3′ untranslated region or the presequence of ATM1 is required for the exclusive localization of its mRNA to the vicinity of mitochondria. Mol. Cell. Biol. *20*, 7881–7892.

Evangelista, M., Blundell, K., Longtine, M.S., Chow, C.J., Adames, N., Pringle, J.R., Peter, M., and Boone, C. (1997). Bni1p, a yeast formin linking Cdc42p and the actin cytoskeleton during polarized morphogenesis. Science *276*, 118–122.

Ferrandon, D., Elphick, L., Nusslein-Volhard, C., and St. Johnston, D. (1994). Staufen protein associates with the 3′UTR of bicoid mRNA to form particles that move in a microtubule-dependent manner. Cell *79*, 1221–1232.

Gonzalez, I., Buonomo, S.B.C., Nasmyth, K., and Von Ahsen, U. (1999). *ASH1* mRNA localization in yeast involves multiple secondary structural elements and Ash1 protein translation. Curr. Biol. *9*, 337–340.

Haarer, B.K., Petzold, A., Lillie, S.H., and Brown, S.S. (1994). Identification of *MYO4*, a second class V myosin gene in yeast. J. Cell Sci. *107*, 1055–1064.

Im, K.H., Cosgrove, D.J., and Jones, A.M. (2000). Subcellular localization of expansin mRNA in xylem cells. Plant Physiol. *123*, 463–470.

Jansen, R.P., Dowzer, C., Michaelis, C., Galova, M., and Nasmyth, K. (1996). Mother cell-specific *HO* expression in budding yeast depends on the unconventional myosin Myo4p and other cytoplasmic proteins. Cell *84*, 687–697.

Jeffrey, W.R., Tomlinson, C.R., and Brodeaur, R.D. (1983). Localization of actin messenger RNA during early ascidian development. Dev. Biol. *99*, 408–417.

Lee, L., Klee, S.K., Evangelista, M., Bonne, C., and Pellman, D. (1999). Control of mitotic spindle position by the *Saccharomyces cerevisiae* formin Bni1p. J. Cell Biol. *144*, 947–961.

Long, R.M., Gu, W., Lorimer, E., Singer, R.H., and Chartrand, P. (2000). She2p is a novel RNA-binding protein that recruits the Myo4p-She3p complex to ASH1 mRNA. EMBO J. *19*, 6592–6601.

Long, R.M., Gu, W., Meng, X., Gonzalvez, G., Singer, R.H., and Chartrand, P. (2001). An exclusively nuclear RNA-binding protein affects asymmetric localization of *ASH1* mRNA, and Ash1p in yeast. J. Cell Biol. *153*, 307–318.

Long, R.M., Singer, R.H., Meng, X., Gonzalez, I., Nasmyth, K., and Jansen, R.-P. (1997). Mating type switching in yeast controlled by asymmetric localization of *ASH1* mRNA. Science *277*, 383–387.

Maxon, M.E., and Herskowitz, I. (2001). Ash1p is a site-specific DNA-binding protein that actively represses transcription. Proc. Natl. Acad. Sci. USA *98*, 1495–1500.

Michaelis, C., Ciosk, R., and Nasmyth, K. (1997). Cohesins: chromosomal proteins that prevent premature separation of sister chromatids. Cell *91*, 35–45.

Miller, R., Matheos, D., and Rose, M. (1999). The cortical localization of the microtubule orientation protein, Kar9p, is dependent upon actin and proteins required for polarization. J. Cell Biol. *144*, 963–975.

Miller, R.K., and Rose, M.D. (1998). Kar9p is a novel cortical protein required for cytoplasmic microtubule orientation in yeast. J. Cell Biol. *140*, 377–390.

Munchow, S., Sauter, C., and Jansen, R.P. (1999). Association of the class V myosin Myo4p with a localized messenger RNA in budding yeast depends on She proteins. J. Cell Sci. *112*, 1511–1518.

Ozaki-Kuroda, K., Yamamoto, Y., Nohara, H., Kinoshita, M., Fujiwara, T., Irie, K., and Takai, Y. (2001). Dynamic localization, and function of Bni1p at the sites of directed growth in *Saccharomyces cerevisiae*. Mol. Cell. Biol. *21*, 827–839.

Peabody, D.S. (1990). Translational repression by bacteriophage MS2 coat protein expressed from a plasmid. J. Biol. Chem. *265*, 5684–5689.

Peabody, D.S., and Ely, K.R. (1992). Control of translational repression by protein-protein interactions. Nucleic Acids Res. *20*, 1649–1655.

Pringle, J.R., Bi, E., Harkins, H.A., Zahner, J.E., De, V.C., Chant, J., Corrado, K., and Fares, H. (1995). Establishment of cell polarity in yeast. Cold Spring Harb Symp. Quant. Biol. *60*, 729–44.

Pruyne, D., and Bretscher, A. (2000). Polarization of cell growth in yeast. J. Cell Sci. *113*, 571–585.

Pruyne, D.W., Schott, D.H., and Bretscher, A. (1998). Tropomyosin-containing actin cables direct the Myo2p-dependent polarized delivery of secretory vesicles in budding yeast. J. Cell Biol. *143*, 1931–1945.

Robinett, C.C., Straight, A., Li, G., Willhelm, C., Sudlow, G., Murray, A., and Belmont, A.S. (1996). In vivo localization of DNA sequences and visualization of large-scale chromatin organization using Lac operator/repressor recognition. J. Cell Biol. *135*, 1685–1700.

Rook, M.S., Lu, M., and Kosik, K. (2000). CaMKIIα 3′ untranslated region-directed mRNA translocation in living neurons: visualization by GFP Linkage. J. Neurosci. *20*, 6385–6393.

Schnall, R., Mannhaupt, G., Stucka, R., Tauer, R., Ehnle, S., Schwarzlose, C., Vetter, I., and Feldmann, H. (1994). Identification of a set of yeast genes coding for a novel family of putative ATPases with high similarity to constituents of the 26S protease complex. Yeast *10*, 1141–1155.

Segal, M., Bloom, K., and Reed, S.I. (2000). Bud6 directs sequential microtubule interactions with the bud tip and bud neck during spindle morphogenesis in *Saccharomyces cerevisiae*. Mol. Biol. Cell *11*, 3689–3702.

SenGupta, D.J., Zhang, B., Kraemer, B., Pochart, P., Fields, S., and Wickens, M. (1996). A three-hybrid system to detect RNA-protein interactions in vivo. Proc. Natl. Acad. Sci. USA *93*, 8496–8501.

Shaw, S.L., Yeh, E., Bloom, K., and Salmon, E.D. (1997). Imaging green fluorescent protein fusion proteins in *Saccharomyces cerevisiae*. Curr. Biol. *7*, 701–704.

Sil, A., and Herskowitz, I. (1996). Identification of asymmetrically localized determinant, Ash1p, required for lineage-specific transcription of the yeast HO gene [see comments]. Cell *84*, 711–722.

St. Johnston, D. (1995). The intracellular localization of messenger RNAs. Cell *81*, 161–170.

Stripecke, R., Oliveira, C.C., McCarthy, J.E.G., and Hentze, M.W. (1994). Proteins binding to 5′ untranslated region sites: a general mechanism for translational regulation of mRNAs in human and yeast cells. Mol. Cell. Biol. *14*, 5898–5909.

Takizawa, P., DeRisi, J., Wilhelm, J., and Vale, R. (2000). Plasma membrane compartmentalization in yeast by messenger RNA transport and a septin diffusion barrier. Science *290*, 341–344.

Takizawa, P.A., Sil, A., Swedlow, J.R., Herskowitz, I., and Vale, R.D. (1997). Actin-dependent localization of an RNA encoding a cell-fate determinant in yeast. Nature *389*, 90–93.

Takizawa, P.A., and Vale, R.D. (2000). The myosin motor, Myo4p, binds Ash1 mRNA via the adapter protein, She3p. Proc. Natl. Acad. Sci. USA *97*, 5273–5278.

Theurkauf, W.E., and Hazelrigg, T.I. (1998). In vivo analyses of cytoplasmic transport and cytoskeletal organization during *Drosophila* oogenesis: characterization of a multi-step anterior localization pathway. Development *125*, 3655–3666.

Uetz, P., Giot, L., Cagney, G., Mansfield, T.A., Judson, R.S., Knight, J.R., Lockshon, D., Narayan, V., Srinivasan, M., Pochart, P., Qureshi-Emili, A., Li, Y., Godwin, B., Conover, D., Kalbfleisch, T., Vijayadamodar, G., Yang, M., Johnston, M., Fields, S., and Rothberg, J.M. (2000). A comprehensive analysis of protein-protein interactions in *Saccharomyces cerevisiae*. Nature *403*, 623–627.

Vale, R.D. (2000). AAA proteins. Lords of the ring. J. Cell Biol. *150*, F13-9.

Wach, A., Brachat, A., Pohlmann, R., and Philippsen, P. (1994). New heterologous modules for classical or PCR-based gene disruptions in *Saccharomyces cerevisiae*. Yeast *10*, 1793–1808.

Wendland, B., McCaffery, J.M., Xiao, Q., and Emr, S.D. (1996). A novel fluorescence-activated cell sorter-based screen for yeast endocytosis mutants identifies a yeast homologue of mammalian eps15. J. Cell Biol. *135*, 1485–500.

Wilhelm, J.E., Mansfield, J., Hom-Booher, N., Wang, S., Turck, C.W., Hazelrigg, T., and Vale, R.D. (2000). Isolation of a ribonucleoprotein complex involved in mRNA localization in *Drosophila* oocytes. J. Cell Biol. *148*, 427–440.

Yeh, E., Yang, C., Chin, E., Maddox, P., Salmon, E.D., Lew, D.J., and Bloom, K. (2000). Dynamic positioning of mitotic spindles in yeast. Role of microtubule motors and cortical determinants. Mol. Biol. Cell *11*, 3949–3961.

Yin, H., Pruyne, D., Huffaker, T.C., and Bretscher, A. (2000). Myosin V orients the mitotic spindle in yeast. Nature *406*, 1013–1015.